Journal of Inflammation Research

Dovepress
Taylor & Francis Group

Open Access Full Text Article

ORIGINAL RESEARCH

Gut Microbiota Characteristics in Acute Pancreatitis Patients and Their Association with SIRS and Organ Failure: An Experimental Study

Qian Wang[1,*], Kaikai Zhang[2,*], Ziyi Ding[1], Guangxiong Si[1], Feng Shen[1], Shanshan Yu[3]

[1]Department of Critical Care Medicine, The Affiliated Hospital of Guizhou Medical University, Guiyang, People's Republic of China; [2]Department of Emergency, The Affiliated Jinyang Hospital of Guizhou Medical University, Guiyang Second People's Hospital, Guiyang, People's Republic of China; [3]Department of Neuro Intensive Care Unit, The Affiliated Jinyang Hospital of Guizhou Medical University, Guiyang Second People's Hospital, Guiyang, People's Republic of China

*These authors contributed equally to this work

Correspondence: Shanshan Yu, Department of Neuro Intensive Care Unit, The Affiliated Jinyang Hospital of Guizhou Medical University, Guiyang Second People's Hospital, No. 547 Jinyang South Road, Guanshanhu District, Guiyang, 550023, People's Republic of China, Email yss_yt0851@163.com

Background: Acute pancreatitis (AP) is a common gastrointestinal disease. Systemic inflammatory response syndrome (SIRS), a severe complication of AP, increases the risk of organ failure and progression to severe AP (SAP). Gut microbiota dysbiosis is linked to AP pathogenesis. The aim of this study is to investigate the gut microbiota characteristics of AP patients and their association with SIRS and organ failure.

Methods: Rectal swabs from 19 healthy controls (HC) and 88 AP patients (stratified into non_SIRS, SIRS, low/med/high_sequential organ failure assessment (SOFA) groups) were analyzed using 16S rRNA gene sequencing. Microbiota diversity, composition, and function were evaluated, and random forest diagnostic models were constructed.

Results: Compared with HC, AP (SIRS/non_SIRS) patients had altered clinical indices, reduced gut microbial richness and diversity. As SOFA scores increased, the high_SOFA group exhibited further reductions in richness and diversity. Barplots analysis showed that there were differences in the mainly dominant microbiota between HC and AP (SIRS/non_SIRS) patients. Some differentially abundant genera such as *Faecalibacterium, Parabacteroides, Megasphaera*, and *Fusicatenibacter* may be closely associated with the occurrence of AP, development of SIRS, and severity of organ failure. Furthermore, functional pathways like L-isoleucine biosynthesis, lysine biosynthesis, AMPK signaling, and glycogen biosynthesis may also play significant roles in diseases. The random forest models constructed for distinguishing between HC and non_SIRS, as well as for distinguishing between HC and SIRS, showed extremely diagnostic accuracy.

Conclusion: Gut microbiota dysbiosis is correlated with the occurrence of AP, development of SIRS, and severity of organ failure. Specific microbiota taxa and functional pathways may serve as potential therapeutic targets or diagnostic biomarkers for AP, providing a microbial perspective for personalized management of this disease.

Keywords: acute pancreatitis, systemic inflammatory response syndrome, sequential organ failure assessment, gut microbiota, function prediction, diagnostic classification model

Introduction

Acute pancreatitis (AP) refers to an acute inflammatory condition of the pancreas.[1] As one of the most common gastrointestinal diseases today, its incidence is continuously increasing across the world and all age groups.[2] Systemic inflammatory response syndrome (SIRS) is a common and serious complication of AP.[3] Persistent SIRS elevates the risk of persistent organ failure and may lead to the progression of AP to severe AP (SAP).[4] SIRS is a key factor in the progression of SAP, and it is closely related to the severity of SAP, which can lead to multiple organ failure and even death.[5–7] The mortality rate of AP increases as much as 30% when organ failure occurs.[8] To accurately assess the

Received: 7 August 2025
Accepted: 19 November 2025
Published: 13 December 2025

severity of organ failure in AP patients with SIRS, the sequential organ failure assessment (SOFA) score has been widely adopted.[9,10] Given that the persistence of SIRS will significantly increase the risk of organ failure and worsen AP outcomes, revealing the influencing mechanism has become the focus of clinical research.

Gut homeostasis is disturbed during the pathogenesis of AP, which can lead to gut microbiota imbalance.[11] In recent years, accumulating evidence has highlighted the role of gut microbiota in the pathogenesis of AP.[12,13] Gut microbiota dysbiosis is linked to enhanced intestinal barrier permeability, bacterial translocation, and amplification of systemic inflammation, thereby influencing AP progression.[14] Derivatives of the gut microbiota can regulate the severity of AP by modulating relevant signaling pathways.[15] Moreover, modulating gut microbiota may indirectly protect the intestinal barrier, alleviating bacterial translocation and inflammatory flare-ups during AP.[16] While existing studies confirm a link between gut microbiota dysbiosis and AP, specific associations between gut microbial characteristics and SIRS occurrence, as well as organ failure severity (as measured by SOFA scores) in AP patients, remain unclear. Moreover, it is not clear which specific microbial taxa or functional pathways are associated with the SIRS progression or organ failure in AP. Thus, the aim of this study is to investigate the gut microbiota characteristics of AP patients and their association with SIRS and organ failure.

Rectal swabs, as a non-invasive sample source, have been increasingly used to characterize gut microbiota composition via 16S rRNA gene sequencing, a technique that enables comprehensive analysis of microbial community structure.[17,18] In this study, rectal swab samples were collected from 19 healthy control volunteers and 88 patients with AP. Subsequently, 16S rRNA gene sequencing technology was used to investigate the composition of the gut microbiome in each group.

Materials and Methods

Patient Selection and Grouping

The detailed inclusion criteria for patients with AP were as follows: (1) Patients diagnosed with AP according to the 2012 revised Atlanta classification and hospitalized in the Affiliated Hospital of Guizhou Medical University; (2) Patients with complete clinical data; (3) Patients who have not received enema treatment; (4) Aged 18–75 years; (5) Onset time within 72 hours. The detailed exclusion criteria for patients with AP were as follows: (1) Patients with a history of immunodeficiency, allergy, asthma, celiac disease, colon cancer, HIV infection, inflammatory bowel disease, irritable bowel syndrome, gastroenteritis, narcotic enterocolitis, or arthritis; (2) Patients who had received antibiotics, probiotics, hormones, traditional Chinese medicine enemas, or other treatments within 8 weeks (8 weeks is a conservative and commonly used time window to exclude the acute effects of potent interventions[19,20]); (3) Patients with missing clinical data; (4) Pregnant women. The control group consisted of healthy individuals with no known allergens, no medication affecting intestinal function, and no special diet for weight loss or other purposes. A power analysis for balanced one-way ANOVA was performed using the pwr package in R, with parameters set as k=3 (number of groups), f=0.5 (effect size), sig.level=0.05 (significance level), and power=0.8 (power level). The results showed that the number of samples required for each group was 14. From January 2025 to May 2025, all patients who were diagnosed with AP according to the 2012 Revised Atlanta Classification, hospitalized at the Affiliated Hospital of Guizhou Medical University, and met the aforementioned inclusion and exclusion criteria were enrolled in this study. This study included a total of 107 participants: 58 patients with AP and SIRS (SIRS group), 30 AP patients without SIRS (non_SIRS group), and 19 healthy control volunteers (HC group). Within the clinically more severe SIRS group, we stratified subgroups based on SOFA scores: low_SOFA (SOFA < 2, n = 20), med_SOFA (SOFA = 2, n = 18), and high_SOFA (SOFA > 2, n = 20). The sample types were rectal swabs.

Illumina MiSeq Sequencing

DNA was extracted from rectal swab samples and detected using 1% agarose gel electrophoresis. The V3–V4 region of the bacteria's 16S ribosomal RNA (rRNA) gene was amplified by PCR using transGen AP221-02: TransStart Fastpfu DNA Polymerase. The PCR instrument was the ABI GeneAmp® 9700. AxyPrep DNA Gel Extraction Kit (AXYGEN) was suitable for gel extraction of PCR products. The QuantiFluor™-ST Blue Fluorescence Quantitation System

(Promega) was used for the quantitation of PCR products. The TruSeq™ DNA Sample Prep Kit was used to process amplification products into standardized library that met the requirements of the Illumina MiSeq sequencing platform.

Sequencing Data Processing

Raw data obtained by MiSeq sequencing were saved in fastq format. FASTP (v0.23.4) and FLASH (v1.2.11) were used to quality-control, filter, and splice of the raw data. Z-Score normalization was performed on the processed data. These processed sequences were subjected to operational taxonomic unit (OTU) analysis. The Usearch (v7.0.1090) was used to cluster OTUs (97% similarity), including extracting non-redundant sequences, removing singletons, and eliminating chimeras. To obtain the species classification information corresponding to each OTU, the RDP classifier (a naive Bayesian classifier) algorithm (version 2.11) was used to perform taxonomic analysis on the OTU representative sequences at the 97% similarity level. The classification confidence was 0.7. Species annotation (reference database: Silva138, https://www.arb-silva.de/documentation/release-138/) was carried out the based on QIIME platform (http://qiime.org/scripts/assign_taxonomy.html).

Diversity Analysis

The mothur package (version 1.30.2) was used for alpha diversity analysis. In alpha diversity, the sobs, chao, and ace indices were used to reflect community richness; the shannon index was used to reflect community diversity; the coverage index was used to reflect community coverage; and the smithwilson index was used to reflect community evenness. The Kruskal–Wallis rank sum test was used to analyze differences of alpha diversity indices among groups. Subsequently, beta diversity analysis was performed using the principal co-ordinates analysis (PCoA) method to investigate the similarities or differences of sample community composition. The unweighted UniFrac distance algorithm was used to calculate the distance between samples. The ANOSIM was used to test differences among groups. In addition, the microbial dysbiosis index (MDI)[21] was calculated using the vegan (v2.4.3) and python (v2.7.10) packages. The larger the MDI value, the higher the degree of microbiota dysbiosis. The Kruskal–Wallis rank sum test was used to analyze differences of MDI among groups.

Composition and Differential Analyses of Microbiota

Barplots were generated using R software (v3.3.1) to illustrate the relative abundance composition of microbial communities at three taxonomic levels (phylum, genus, and species) in all study groups. Meanwhile, differential abundance analysis was conducted using the stats in the R package (v3.3.1). Based on the relative abundance data of community, the Wilcoxon rank-sum test was used to identify gut microbiota with significant differences between groups ($P < 0.05$).

Function Prediction

PICRUSt2 is an important tool for predicting the functions of microbial community using 16S rRNA gene data.[22] Its predictions are based on several gene family databases, including MetaCyc and Kyoto Encyclopedia of Genes and Genomes (KEGG).[23] KEGG is an integrated database resource composed of multiple functional units such as enzyme, KEGG module, and KEGG pathway.[24] MetaCyc database is the largest curated collection of metabolic pathways.[25] In this study, PICRUSt2 (http://huttenhower.sph.harvard.edu/galaxy) was used for functional prediction, and the Kruskal–Wallis rank sum test was employed to analyze differences among groups.

Construction of Diagnostic Models

The randomForest function in the R package (v3.3.1) was used to construct random forest diagnostic classification models. Genus level microbiota taxa were ranked by importance in descending order based on the Mean Decrease Accuracy value derived from the random forest algorithm. Following the ranking results, taxa were added one by one in top-to-bottom order. For each of these cases, classification was conducted via the random forest algorithm, and the area under curve (AUC) value was calculated using the 10-fold cross-validation. The genera involved when the AUC value reached its maximum were identified as the optimal biomarkers. The pROC in the R package (v3.3.1) was used to

perform receiver operator characteristic (ROC) analysis to verify the diagnostic accuracy of classification models. The AUC ranges from 0 to 1, and it is a good indicator of the goodness of the test. A perfect diagnostic test achieves an AUC of 1.0.[26]

Statistical Analysis

The statistical analyses in this study were performed using R software. Normally distributed continuous variables were expressed as mean ± standard deviation (SD) and analyzed using analysis of variance (ANOVA). Non-normally distributed continuous variables were presented as median (Q_1, Q_3) and compared using the Kruskal–Wallis test. Categorical variables were expressed as frequencies (percentages) and analyzed using either the chi-square test or Fisher's exact test, as appropriate. $P < 0.05$ was considered statistically significant.

Results

Statistical Analysis of Clinical Characteristics

Among the SIRS, non_SIRS, and HC groups, there were no significant differences in demographic indicators such as age, body mass index (BMI), and gender. However, significant differences were observed in drinking history, smoking history, and hypertension, suggesting that drinking history, smoking history, and hypertension may be risk factors for disease. Among clinical indicators, the neutrophil percentage and count (NEU%, NEU#) in the SIRS group were significantly higher than those in the non_SIRS group, while the lymphocyte count (LYM#) was significantly lower. Additionally, scores such as SOFA and acute physiology and chronic health evaluation II (APACHE II), as well as serum amylase (AMS) levels, were higher in the SIRS group (Table S1), indicating a more severe inflammatory response and condition in the SIRS group.

Fifty-eight patients with SIRS were further divided into three groups based on their SOFA scores: low_SOFA, med_SOFA, and high_SOFA. The high_SOFA group had significantly lower platelets (Plt) and significantly higher levels of D-dimer, serum creatinine (Cr), aspartate aminotransferase (AST), and alanine aminotransferase (ALT), suggesting more obvious organ damage. Moreover, the proportion of severe acute pancreatitis (SAP) in the high_SOFA group was 45.00%, higher than the 10.00% in the low_SOFA group, indicating that higher SOFA scores were associated with greater disease severity (Table S2).

Differences in inflammatory factors among different groups were also compared. The results showed that the non_SIRS group had significantly lower levels of white blood cells (WBC), systemic immune-inflammation index (SII), systemic inflammatory response index (SIRI), C-reactive protein (CRP), procalcitonin (PCT), and interleukin-6 (IL-6) compared to the SIRS-related subgroups (low_SOFA, med_SOFA, and high_SOFA). Among the SIRS subgroups, the high_SOFA group had significantly higher levels of CRP and PCT than the low_SOFA and med_SOFA groups, and IL-6 levels were also higher than those in the latter two groups (Table 1). These findings suggest that inflammatory factor levels were directly correlated with disease severity, with the high_SOFA group exhibiting the most intense inflammatory response.

Table 1 Blood Concentrations of Inflammatory Factors in Different Subgroups of Patients with Acute Pancreatitis

Variables	Low_SOFA	Med_SOFA	High_SOFA	Non_SIRS	F/H	P
WBC	15.24 ± 4.60	15.40 ± 4.40	14.31 ± 5.05	10.22 ± 2.62[abc]	9.066	<0.001
SII	3463.12 ± 2232.36	2685.50 ± 1676.01	3195.59 ± 3276.29	1384.10 ± 1051.96[abc]	4.89	0.004
SIRI	10.29 ± 6.85	9.90 ± 7.85	11.23 ± 9.17	3.48 ± 3.12[abc]	7.246	<0.001
CRP	106.42 ± 92.88	149.00 ± 110.99	201.75 ± 125.79[a]	45.20 ± 53.94[abc]	10.623	<0.001
PCT	0.11 (0.07, 0.32)	0.12 (0.07, 0.84)	2.04 (0.48, 9.49)[ab]	0.08 (0.04, 0.11)[c]	39.229	<0.001
IL-6	79.40 (24.80, 169.25)	88.10 (22.75, 175.40)	117.50 (68.40, 213.20)	9.40 (4.10, 20.65)[abc]	32.813	<0.001

Notes: [a]Represents P < 0.05 vs low_SOFA. [b]Represents P < 0.05 vs med_SOFA. [c]Represents P < 0.05 vs high_SOFA.
Abbreviations: WBC, White Blood Cell; SII, Systemic immune-inflammation index; SIRI, Systemic inflammatory response index; CRP, C-reactive protein; PCT, Procalcitonin; IL-6, Interleukin-6.

Diversity Analysis of Microbiota

Compared with the HC group, the ace, chao, sobs and shannon indexes were significantly decreased in the SIRS and non_SIRS groups (Figure 1A–D), while the coverage and smithwilson indexes were significantly increased (Figure 1E and F). These results suggested that microbial richness may be reduced in the disease state, and the community structure may also have undergone changes. However, there were no significant differences in community richness, community diversity, community coverage and community evenness between the SIRS and non_SIRS groups. Moreover, with the increase of SOFA scores, the high_SOFA group showed decreased community richness and community diversity, as well as increased community coverage and community evenness (Figure 1G–L). Among them, compared with the low_SOFA group, the differences in community richness and community coverage were statistically significant.

PCoA analysis showed that distinct differences existed in the distribution patterns between the HC and SIRS groups, as well as between the HC and non_SIRS groups. Meanwhile, an overlap was observed between the SIRS and non_SIRS groups (Figure S1A). This indicated that the microbiota structure of both the SIRS group and the non_SIRS group were notably different from that of the HC group, while the microbiota structure of the SIRS and non_SIRS groups was not significantly different. The sample distributions among the low_SOFA, med_SOFA, and high_SOFA groups were somewhat dispersed (Figure S1B). The P value also indicated that there were certain differences among the groups. However, the degree of difference in microbiota structure among the groups was relatively small. MDI results indicated that the microbial dysbiosis in SIRS and non_SIRS groups were relatively severe (Figure S1C). Additionally, as the SOFA score increased, the microbial dysbiosis worsened (Figure S1D).

Composition of Microbiota in Different Groups

Barplot revealed that the mainly dominant microbiota in the HC group at the phylum level were Bacillota, Bacteroidota, Actinomycetota, and Pseudomonadota (Figure 2A). The mainly dominant microbiota in the SIRS, non_SIRS, low_SOFA, med_SOFA, and high_SOFA groups at the phylum level were Bacillota, Bacteroidota, Pseudomonadota, and Fusobacteriota (Figure 2A and B). At the genus level, barplot showed that the mainly dominant microbiota in the HC group were *Blautia, Bacteroides, Faecalibacterium, Segatella*, and *Agathobacter* (Figure 2C). The mainly dominant

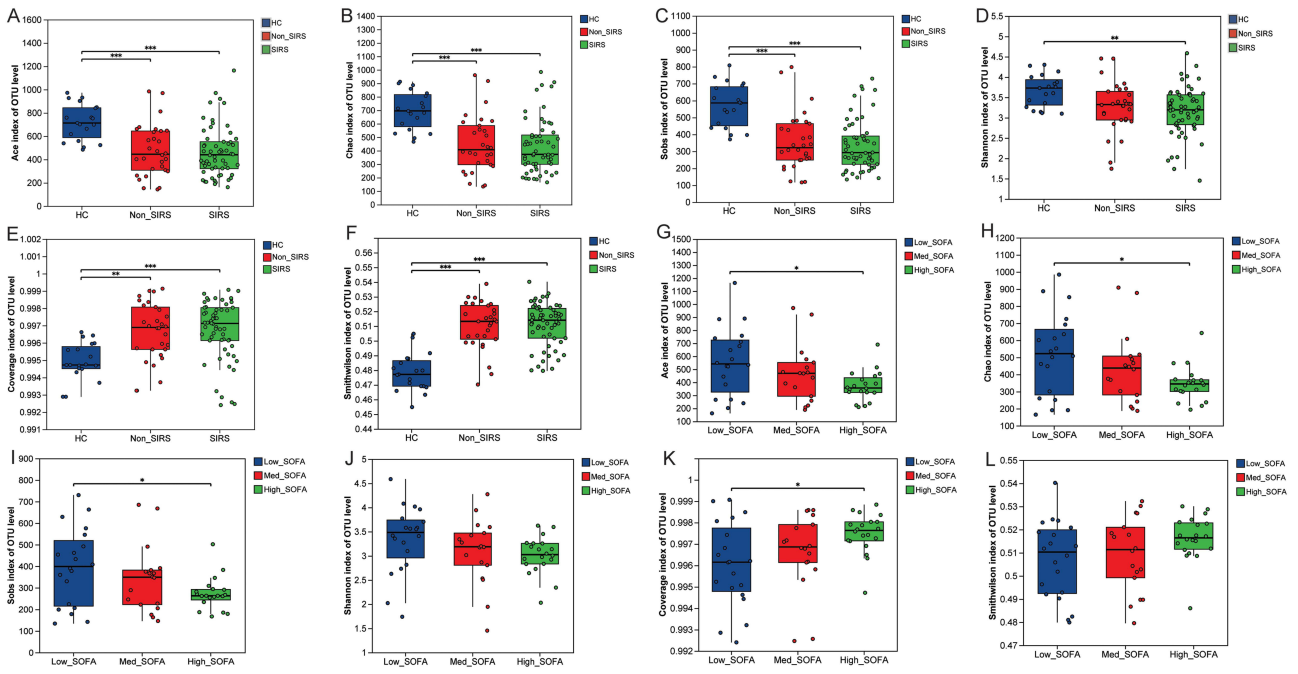

Figure 1 Alpha diversity analysis. (**A**–**F**) Difference analysis of ace, chao, sobs, shannon, coverage, and smithwilson indexes among the HC, SIRS, and non_SIRS groups; (**G**–**L**) Difference analysis of ace, chao, sobs, shannon, coverage, and smithwilson indexes among the low_SOFA, med_SOFA, and high_SOFA groups. *P <0.05; **P <0.01; ***P <0.001. Kruskal–Wallis rank sum test.

https://doi.org/10.2147/JIR.S559136

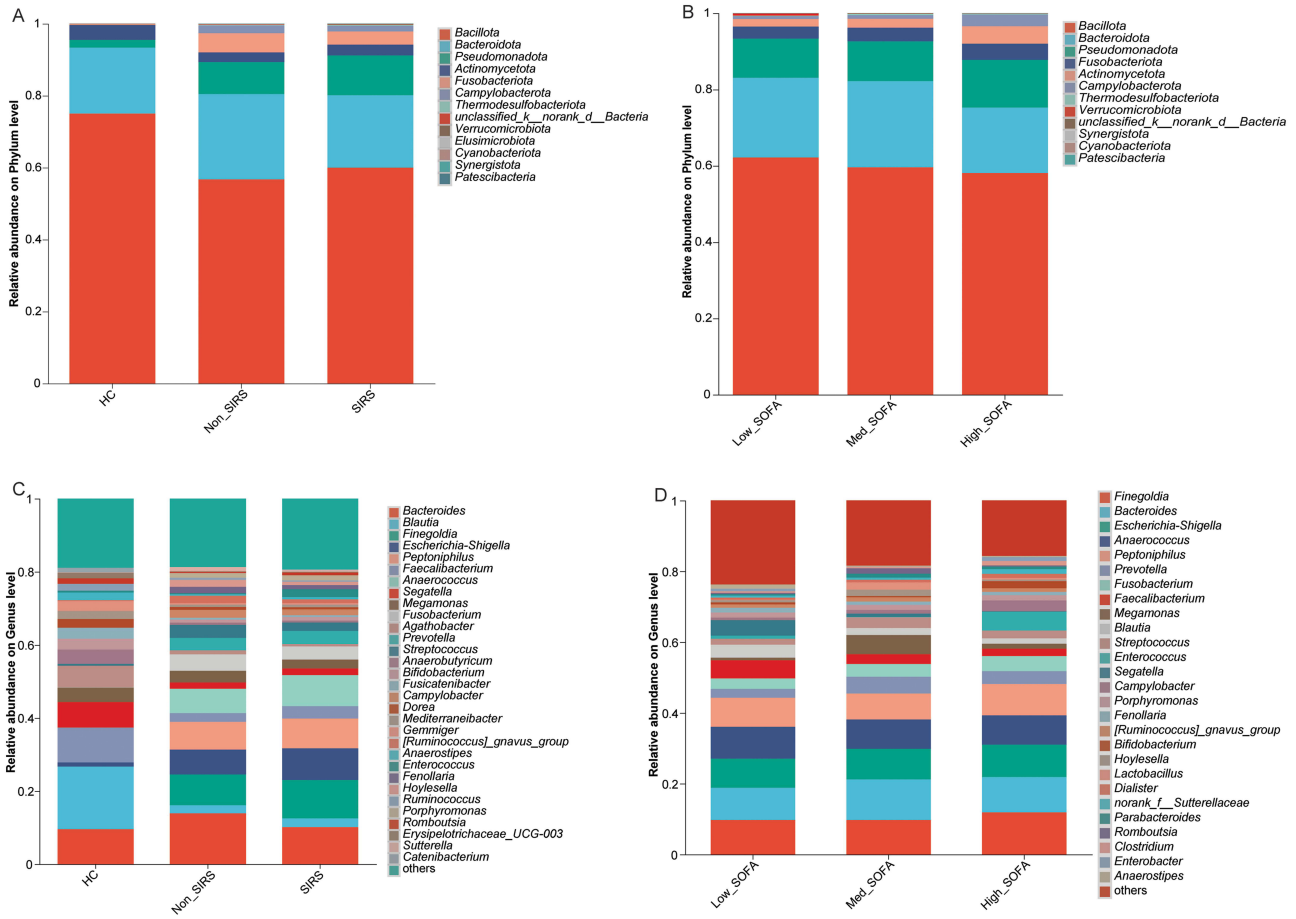

Figure 2 Barplots of the dominant microbiota species at phylum and genus levels in different groups. (**A**) Barplot of the dominant species at phylum level in the HC, SIRS, and non_SIRS groups; (**B**) Barplot of the dominant species at phylum level in the low_SOFA, med_SOFA, and high_SOFA groups; (**C**) Barplot of the dominant species at genus level in the HC, SIRS, and non_SIRS groups; (**D**) Barplot of the dominant species at genus level in the low_SOFA, med_SOFA, and high_SOFA groups.

microbiota in the SIRS, non_SIRS, low_SOFA, med_SOFA, and high_SOFA groups at the genus level were *Bacteroides, Finegoldia, Peptoniphilus, Escherichia-Shigella*, and *Anaerococcus* (Figure 2C and D). At both the phylum and genus levels, the mainly dominant microbiota in each disease group exhibited consistency, whereas they showed certain differences from those in the HC group, indicating a certain degree of disorder in the microbiota of each disease group.

Differential Analysis of Microbiota at the Genus Level

The Wilcoxon rank sum test identified 94 taxa with significant differences between the HC and non_SIRS groups, including *Blautia, Faecalibacterium, Finegoldia, Escherichia-Shigella*, and *Peptoniphilus* (Figure 3A). It revealed 9 taxa with significant differences between the SIRS and non_SIRS groups, such as *Parabacteroides, norank_uncl. Sutterellaceae* (also known as *norank_f_Sutterellaceae*), *Limosilactobacillus, Winkia*, and *Actinotignum* (Figure 3B). There were 113 taxa with significant differences between the HC and SIRS groups, such as *Blautia, Faecalibacterium, Finegoldia, Escherichia-Shigella*, and *Segatella* (Figure 3C). Additionally, 12 taxa with significant differences were identified between the low_SOFA and med_SOFA, such as *Megasphaera, norank_f__[Eubacterium]_coprostanoligenes_group, Eggerthella, Sellimonas*, and *UCG-003* (Figure 4A). Moreover, 9 taxa with significant differences were identified between the med_SOFA and high_SOFA groups, such as *Fusicatenibacter, Limosilactobacillus, Lachnospira, norank_f__Lachnospiraceae*, and *norank_o__Clostridia_UCG-014* (Figure 4B). The identification of these differential taxa was expected to reveal the mechanisms of action of the microbiota in the occurrence and progression of diseases, thereby providing candidate microbiota for the development of microbiota-based therapeutic strategies.

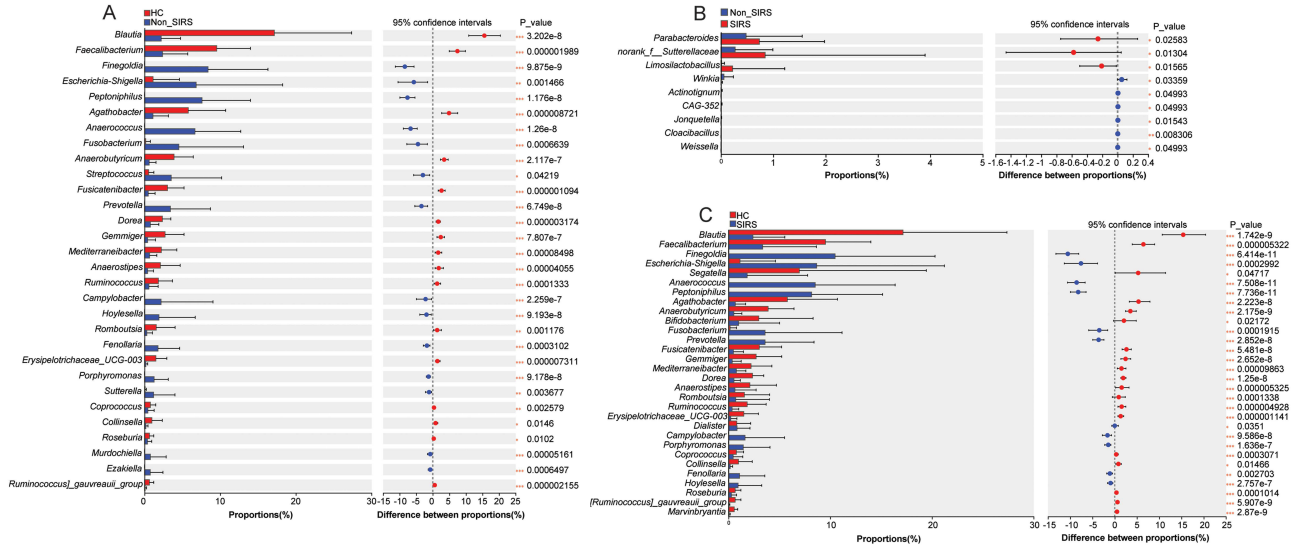

Figure 3 Differential analysis of microbiota at genus level in the HC, SIRS, and non_SIRS groups. (**A**) Differential analysis of microbiota at genus level between the HC and non_SIRS groups; (**B**) Differential analysis of microbiota at genus level between the SIRS and non_SIRS groups; (**C**) Differential analysis of microbiota at genus level between the HC and SIRS groups. *P <0.05; **P <0.01; ***P <0.001. Wilcoxon rank-sum test.

Identification of Differential PICRUSt Functions

Within the functional units of enzyme (Figure 5A), MetaCyc (Figure 5B), module (Figure 5C), and pathway (Figure 5D), significant differences in multiple functional features were observed among the HC, SIRS, and non_SIRS groups. Functions such as 6-phosphofructokinase (Enzyme_ID: 2.7.1.11), PWY-5101: L-isoleucine biosynthesis II, M00527: Lysine biosynthesis, DAP aminotransferase pathway, aspartate ≤ lysine, and 2-Oxocarboxylic acid metabolism were particularly prominent among these differences and may play important roles in the pathological mechanisms of patients. Likewise, within the functional units of enzyme (Figure 6A), MetaCyc (Figure 6B), module (Figure 6C), and pathway (Figure 6D), marked differences in multiple functions were also observed among low_SOFA, med_SOFA, and high_SOFA groups. Functions such as UMP/CMP kinase (Enzyme_ID: 2.7.4.14), GLYCOGENSYNTH-PWY: glycogen biosynthesis I (from ADP-D-Glucose), M00763: Ornithine biosynthesis, mediated by LysW, glutamate ≤ ornithine, and AMPK signaling pathway stood out as typical examples, and they may play a significant role in the progression of the patients' diseases. The results of PICRUSt analysis revealed the potential association between the microbiota and diseases at the functional level, providing a new perspective for understanding the molecular mechanisms of diseases.

Construction of Random Forest Classification Models for HC and non_SIRS Groups, as Well as HC and SIRS Groups Based on Genus Level Microbiota

Random forest analysis was performed on the genus level microbiota of HC and non_SIRS groups. The results showed that the AUC value reached the maximum when the number of included species was two (*Anaerococcus* and *Varibaculum*) (Figure S2A and B). ROC curve analysis indicated that the classification model constructed based on *Anaerococcus* and *Varibaculum* had excellent diagnostic accuracy in distinguishing between the HC and non_SIRS groups (Figure S2C). Similarly, random forest analysis was performed on the genus level microbiota of HC and SIRS groups. The results showed that the AUC value reached the maximum when the number of included species was two (*Peptoniphilus* and *Finegoldia*) (Figure S2D and E). ROC curve analysis indicated that the classification model constructed based on *Peptoniphilus* and *Finegoldia* had excellent diagnostic accuracy in distinguishing between the HC and SIRS groups (Figure S2F). Although these models showed excellent diagnostic accuracy, their clinical value in independent populations still needs to be further verified.

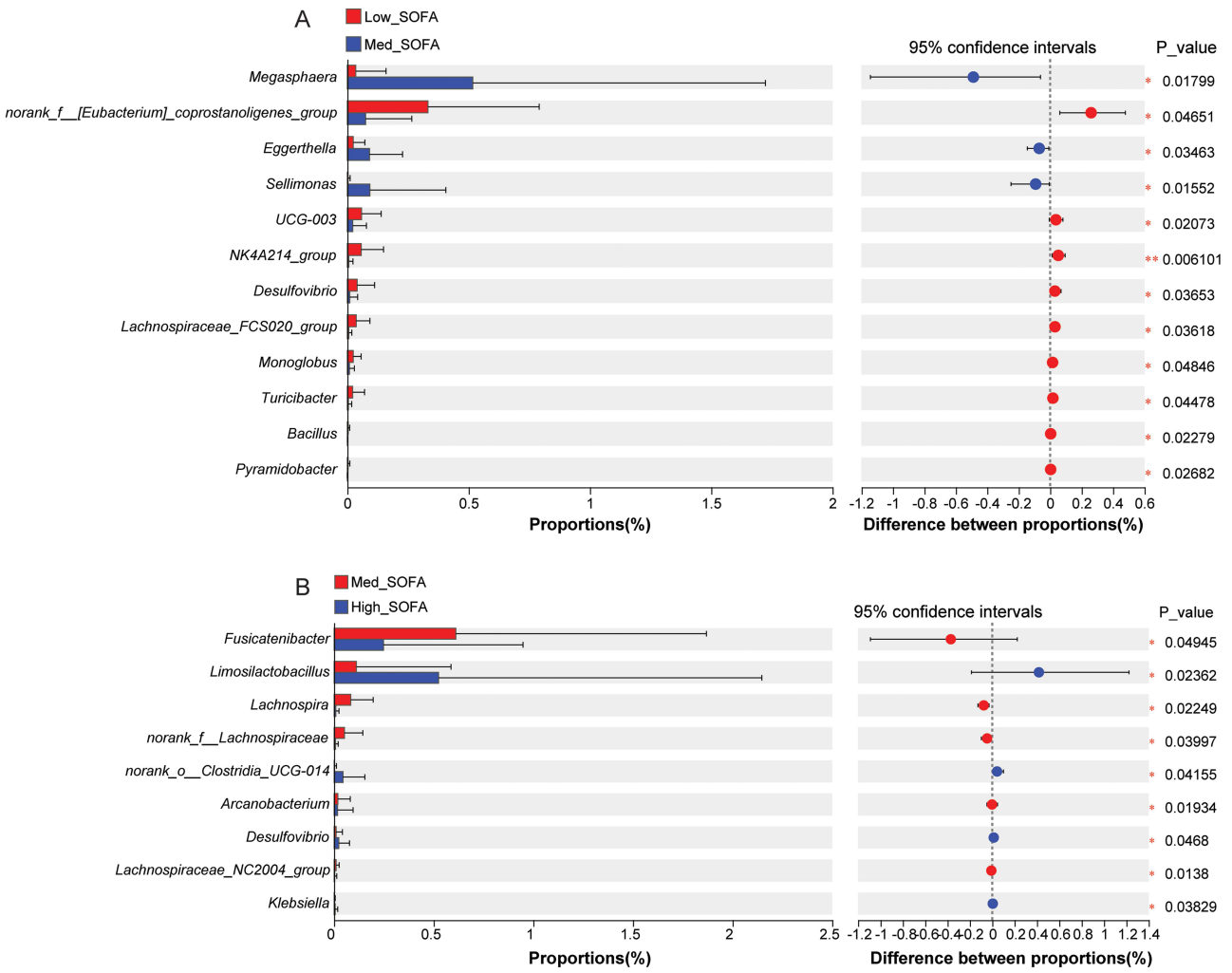

Figure 4 Differential analysis of microbiota at genus level in the low_SOFA, med_SOFA, and high_SOFA groups. (**A**) Differential analysis of microbiota at genus level between the low_SOFA and med_SOFA groups; (**B**) Differential analysis of microbiota at genus level between the med_SOFA and high_SOFA groups. *P <0.05; **P <0.01. Wilcoxon rank-sum test.

Discussion

This study explored the characteristics of gut microbiota in AP patients with or without SIRS, healthy controls, and subgroups stratified by SOFA scores using 16S rRNA gene sequencing of rectal swabs. The results revealed alterations in gut microbiota diversity, composition, and function, which provide new insights into the interplay between gut microbiota and the progression of AP. Clinical data analysis showed that the SIRS group exhibited higher neutrophil, SOFA scores, APACHE II scores, and serum amylase levels, accompanied by elevated inflammatory factors (CRP, PCT, IL-6), which is consistent with the pathological feature that SIRS in AP is driven by excessive systemic inflammation, leading to aggravated organ dysfunction.[4,8] Notably, the high_SOFA group had lower platelets and higher D-dimer, Cr, AST, and ALT, confirming that elevated SOFA scores reflect more severe organ damage.

Alpha diversity analysis demonstrated that compared with the HC group, the SIRS and non_SIRS groups had significantly reduced community richness (ace, chao, sobs) and diversity (shannon), while community coverage and evenness increased. This is consistent with previous findings that AP is accompanied by gut microbiota dysbiosis and a decreased microbial diversity.[27,28] Notably, as SOFA scores increased, the high_SOFA group exhibited further reductions in richness and diversity, indicating that severe organ dysfunction is linked to more pronounced microbiota imbalance. Furthermore, the results of beta diversity analysis showed that there were significant differences in the distribution patterns of microbial communities between HC and AP (SIRS/non_SIRS) groups, which also confirmed the

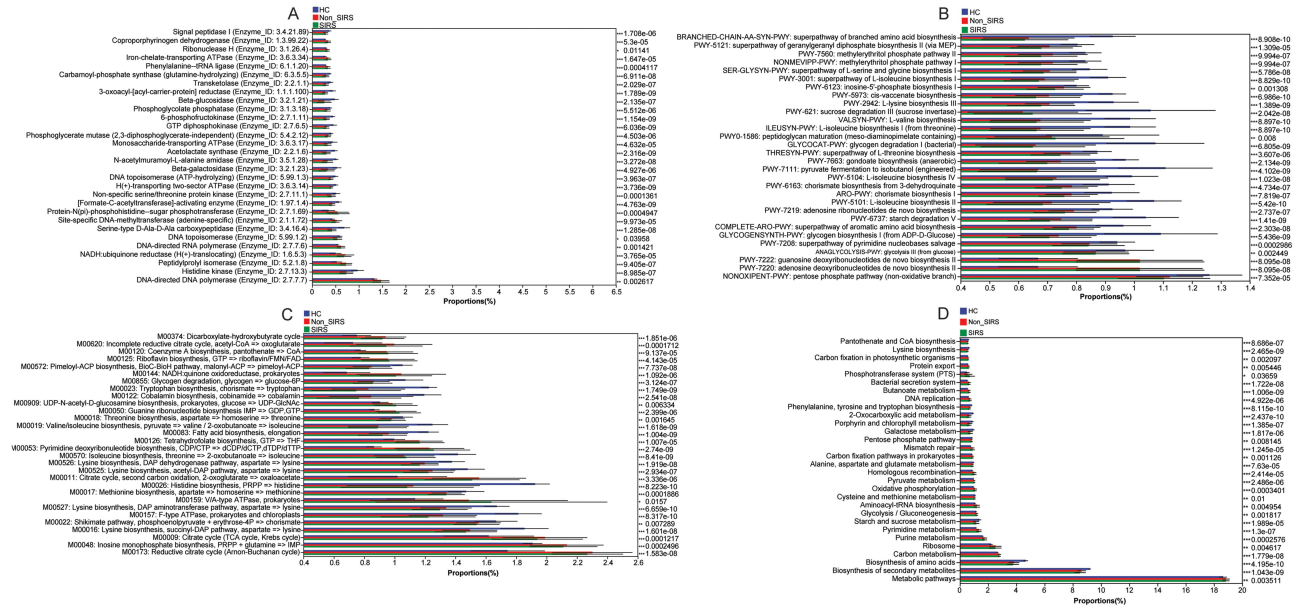

Figure 5 PICRUSt functional prediction of HC, SIRS, and non_SIRS groups. (**A**) Difference analysis of Enzyme functional of microbiota among the HC, SIRS, and non_SIRS groups; (**B**) Difference analysis of MetaCyc functional of microbiota among the HC, SIRS, and non_SIRS groups; (**C**) Difference analysis of KEGG Module functional of microbiota among the HC, SIRS, and non_SIRS groups; (**D**) Difference analysis of KEGG Pathway functional of microbiota among the HC, SIRS, and non_SIRS groups. *P <0.05; **P <0.01; ***P <0.001. Kruskal–Wallis rank sum test.

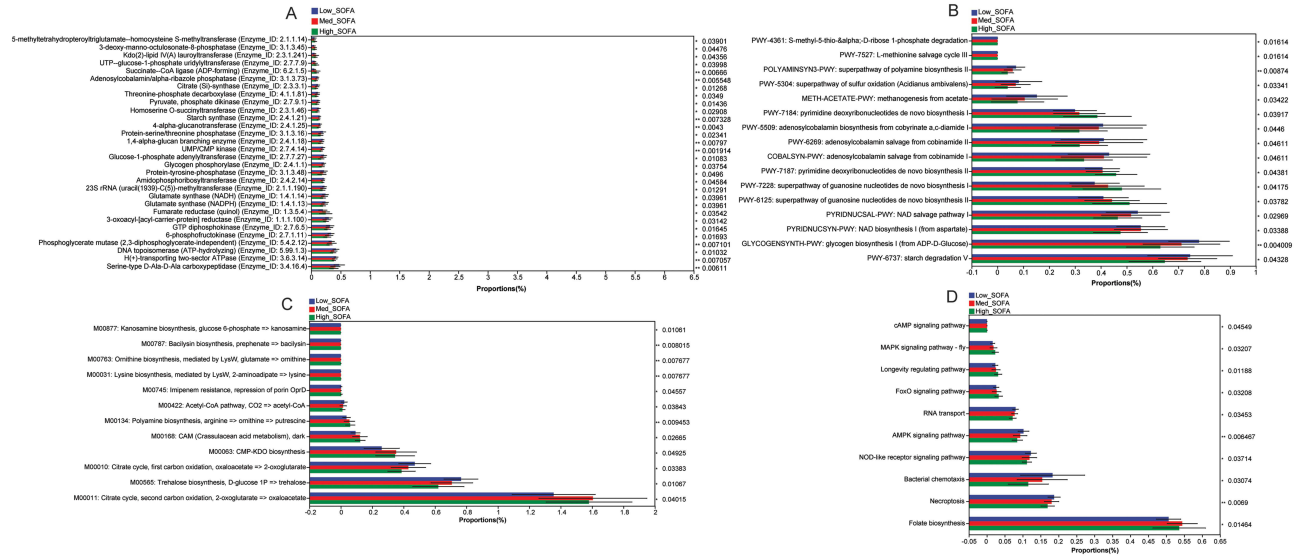

Figure 6 PICRUSt functional prediction of low_SOFA, med_SOFA, and high_SOFA groups. (**A**) Difference analysis of Enzyme functional of microbiota among the low_SOFA, med_SOFA, and high_SOFA groups groups; (**B**) Difference analysis of MetaCyc functional of microbiota among the low_SOFA, med_SOFA, and high_SOFA groups groups; (**C**) Difference analysis of KEGG Module functional of microbiota among the low_SOFA, med_SOFA, and high_SOFA groups groups; (**D**) Difference analysis of KEGG Pathway functional of microbiota among the low_SOFA, med_SOFA, and high_SOFA groups groups. *P <0.05; **P <0.01; ***P <0.001. Kruskal–Wallis rank sum test.

importance of microbial community structure in the occurrence of AP. However, there were no significant differences in the alpha and beta diversity between the SIRS and non_SIRS groups. This may suggest that the microbial communities in the SIRS and non_SIRS groups are relatively stable in terms of diversity, evenness, coverage and the degree of change in community composition. The MDI further confirmed that patients with AP have more severe microbiota disorder, and MDI increases with SOFA scores, reinforcing the correlation between microbiota dysregulation and disease severity.

https://doi.org/10.2147/JIR.S559136

Barplots showed that there were differences in the mainly dominant microbiota between HC and AP patients, especially at the genus level. The mainly dominant microbiota in the HC individuals at the genus level were *Blautia, Bacteroides, Faecalibacterium, Segatella*, and *Agathobacter*. The mainly dominant microbiota in the AP patients at the genus level were *Bacteroides, Finegoldia, Peptoniphilus, Escherichia-Shigella*, and *Anaerococcus*. *Blautia* is a genus of anaerobic bacteria with probiotic properties, and it plays a significant role in alleviating inflammatory and metabolic diseases.[29] *Faecalibacterium* is a genus of strictly anaerobic, extremely oxygen-sensitive. Low level of *Faecalibacterium* is associated with inflammation.[30] One of the main metabolites produced by *Faecalibacterium* is butyrate,[31] which can be used as a carbon source by colon cells and enhances the intestinal barrier by strengthening tight junctions.[32] A study has shown that GV-971 can promote *Faecalibacterium*, resulting in subsequent anti-inflammatory microbiota metabolites (such as propionate and butyrate) that inhibit macrophage M1 polarization in SAP.[33] *Agathobacter* is a beneficial bacterium in the gastrointestinal tract, and its reduced abundance is associated with many neurological diseases and mediates neuroinflammation.[34] *Agathobacter* is also associated with extraintestinal manifestations of inflammatory bowel disease.[35] *Finegoldia* and *Peptoniphilus*, as anaerobic gram-positive cocci, are often associated with infections and inflammations.[20,36–38] *Escherichia-Shigella* is the major intestinal microbe in AP, and increased abundance of this group is associated with the deterioration of AP.[12] Members of the genus *Anaerococcus* are mostly anaerobic gram-positive cocci and are closely associated with human health.[39] *Anaerococcus* is also a potential diagnostic biomarker for moderate AP.[20] Moreover, the Wilcoxon rank sum test results showed that *Blautia, Faecalibacterium, Agathobacter, Finegoldia, Peptoniphilus, Escherichia-Shigella*, and *Anaerococcus* exhibited significant differences between the HC and AP (SIRS/non_SIRS) groups, suggesting that they may play an important role in the AP, and the specific mechanism needs further study.

The Wilcoxon rank sum test also revealed 9 significantly different taxa between the SIRS and non_SIRS groups, such as *Parabacteroides, norank_f__Sutterellaceae, Limosilactobacillus, Winkia*, and *Actinotignum*. These taxa are part of the gut microbiota and may be involved in gastrointestinal health and disease. For example, some members of *Parabacteroides* have been associated with the production of short-chain fatty acids, which play important roles in gut health.[40,41] In the context of AP, we hypothesize that they may be associated with the development of SIRS. However, their specific functional mechanisms remain unclear and require further investigation. Additionally, 12 taxa with significant differences were identified between the low_SOFA and med_SOFA, such as *Megasphaera* and *Eggerthella*. Moreover, 9 taxa with significant differences were identified between the med_SOFA and high_SOFA groups, such as *Fusicatenibacter* and *Lachnospira*. In the context of AP, they may be associated with the patient's organ failure. Studies have shown that *Megasphaera*,[42] *Eggerthella*,[43] *Fusicatenibacter*,[44] and *Lachnospira*[45] are closely related to human health, but the role of *Megasphaera, Eggerthella, Fusicatenibacter*, and *Limosilactobacillus* in AP remains to be further studied. This study provides a potential research direction for subsequent exploration.

PICRUSt2 analysis revealed functional differences in gut microbiota among groups. In the comparison among the HC, SIRS, and non_SIRS groups, pathways such as L-isoleucine biosynthesis and lysine biosynthesis were altered. Amino acids are the basic building blocks of protein synthesis, and their metabolic disorders are associated with various pathological conditions, including metabolic diseases, cardiovascular diseases, immune and inflammatory diseases, and cancer.[46] For the SIRS subgroups, there was a significant difference in the enrichment of the AMPK signaling pathway. AMPK is a key regulator of energy metabolism, and its activation can inhibit inflammatory responses.[47,48] Additionally, glycogen biosynthesis pathway was altered among SIRS subgroups, which may be related to the energy metabolism disorder in organ failure.[49] Collectively, these results suggest that gut microbiota-driven functional dysregulation plays a crucial role in the occurrence and progression of AP as well as the severity of AP-related organ failure, providing new insights for subsequent research.

Random forest, a powerful machine learning algorithm that leverages bootstrap aggregation and randomization of predictors for high prediction accuracy, finds extensive use across multiple domains, including the development of diagnostic classification models.[50–53] In this study, the random forest models constructed using *Anaerococcus* and *Varibaculum* (for distinguishing HC and non_SIRS) and *Peptoniphilus* and *Finegoldia* (for distinguishing HC and SIRS) showed excellent diagnostic accuracy, suggesting these genera could serve as potential microbial biomarkers.

From the patient's perspective, the findings of this study have practical implications for the clinical management of AP. In terms of early diagnosis and risk stratification, the microbial biomarkers identified were derived from rectal swabs. This is a non-invasive, easy-to-collect sample that causes minimal discomfort to AP patients. Compared with invasive sampling or complex imaging, rectal swab-based microbial detection is more acceptable to patients and reduces the psychological burden of repeated invasive tests. For prognosis monitoring, the dysregulation of the gut microbiota provides potential "accessible indicators" for the progression of the disease in patients. Combined with routine clinical indicators, microbial changes can help patients and clinicians better understand disease severity, adjust care plans in a timely manner, and improve treatment compliance.

However, this study also has certain limitations. Firstly, the specific mechanism between the identified gut microbiota and the progression of AP remains unclear and requires further investigation via functional experiments (eg, fecal transplantation experiments). Secondly, the current sample size is relatively small, and the constructed diagnostic classification models still need further validation in larger clinical samples. In conclusion, this study demonstrates that gut microbiota dysbiosis is closely associated with the occurrence of AP, development of SIRS, and severity of organ failure. Specific microbiota taxa and functional pathways may serve as potential therapeutic targets or diagnostic biomarkers for AP, providing a microbial perspective for personalized management of this disease.

Abbreviations

AP, Acute pancreatitis; SAP, severe acute pancreatitis; HC, healthy controls; SIRS, Systemic inflammatory response syndrome; SOFA, sequential organ failure assessment; OTU, operational taxonomic unit; PCoA, principal co-ordinates analysis; MDI, microbial dysbiosis index; KEGG, Kyoto Encyclopedia of Genes and Genomes; AUC, area under curve; ROC, receiver operator characteristic; SD, standard deviation; ANOVA, analyzed using analysis of variance; BMI, body mass index; AMS, amylase; Plt, platelets; Cr, creatinine; AST, aspartate aminotransferase; ALT, alanine aminotransferase; WBC, white blood cells; SII, systemic immune-inflammation index; SIRI, systemic inflammatory response index; CRP, C-reactive protein; PCT, procalcitonin; IL-6, interleukin-6.

Data Sharing Statement

The data generated during and/or analysed during the current study are available from the corresponding author on reasonable request.

Ethics Approval and Informed Consent

This study was approved by the Ethics Committee of the Affiliated Hospital of Guizhou Medical University (2025153). This study complied with the Declaration of Helsinki. Written informed consent was obtained from all participants.

Funding

This study was funded by the Guiyang Science and Technology Plan Project (NO. [2024] 2-24).

Disclosure

The authors declare no competing interests in this work.

References

1. Tenner S, Vege SS, Sheth SG, et al. American college of gastroenterology guidelines: management of acute pancreatitis. *Am J Gastroenterol*. 2024;119(3):419–437. doi:10.14309/ajg.0000000000002645
2. Trikudanathan G, Yazici C, Evans Phillips A, Forsmark CE. Diagnosis and management of acute pancreatitis. *Gastroenterology*. 2024;167(4):673–688. doi:10.1053/j.gastro.2024.02.052
3. Zhang R, Zhu S, Shi L, et al. Automated machine learning for early prediction of systemic inflammatory response syndrome in acute pancreatitis. *BMC Med Inform Decis Mak*. 2025;25(1):167. doi:10.1186/s12911-025-02997-7
4. Komara NL, Paragomi P, Greer PJ, et al. Severe acute pancreatitis: capillary permeability model linking systemic inflammation to multiorgan failure. *American J Physiol*. 2020;319(5):G573–g583. doi:10.1152/ajpgi.00285.2020
5. Prajapati R, Manay P, Sugumar K, Rahandale V, Satoskar R. Acute pancreatitis: predictors of mortality, pancreatic necrosis and intervention. *Turk J Surg*. 2021;37(1):13–21. doi:10.47717/turkjsurg.2021.5072

6. Habtezion A, Gukovskaya AS, Pandol SJ. Acute pancreatitis: a multifaceted set of organelle and cellular interactions. *Gastroenterology*. 2019;156(7):1941–1950. doi:10.1053/j.gastro.2018.11.082
7. Boxhoorn L, Voermans RP, Bouwense SA, et al. Acute pancreatitis. *Lancet*. 2020;396(10252):726–734. doi:10.1016/s0140-6736(20)31310-6
8. Schepers NJ, Bakker OJ, Besselink MG, et al. Impact of characteristics of organ failure and infected necrosis on mortality in necrotising pancreatitis. *Gut*. 2019;68(6):1044–1051. doi:10.1136/gutjnl-2017-314657
9. Tee YS, Fang HY, Kuo IM, Lin YS, Huang SF, Yu MC. Serial evaluation of the SOFA score is reliable for predicting mortality in acute severe pancreatitis. *Medicine*. 2018;97(7):e9654. doi:10.1097/md.0000000000009654
10. Zhou J, Wang L, Chen T, et al. Effect of plasmapheresis versus standard medical treatment in patients with hypertriglyceridemia-associated acute pancreatitis complicated by early organ failure (PERFORM-R): study design and rationale of a multicenter, pragmatic, registry-based randomized controlled trial. *Pancreatology*. 2025;25(2):221–227. doi:10.1016/j.pan.2025.01.008
11. Zhu Y, Mei Q, Fu Y, Zeng Y. Alteration of gut microbiota in acute pancreatitis and associated therapeutic strategies. *Biomed Pharmacother*. 2021;141:111850. doi:10.1016/j.biopha.2021.111850
12. Wu L, Hu J, Yi X, et al. Gut microbiota interacts with inflammatory responses in acute pancreatitis. *Therap Adv Gastroenterol*. 2023;16:17562848231202133. doi:10.1177/17562848231202133
13. Lu WW, Chen X, Ni JL, Zhu SL, Fei AH, Wang XS. The role of gut microbiota in the pathogenesis and treatment of acute pancreatitis: a narrative review. *Ann Palliat Med*. 2021;10(3):3445–3451. doi:10.21037/apm-21-429
14. Li XY, He C, Zhu Y, Lu NH. Role of gut microbiota on intestinal barrier function in acute pancreatitis. *World J Gastroenterol*. 2020;26(18):2187–2193. doi:10.3748/wjg.v26.i18.2187
15. Liu LW, Xie Y, Li GQ, et al. Gut microbiota-derived nicotinamide mononucleotide alleviates acute pancreatitis by activating pancreatic SIRT3 signalling. *Br J Pharmacol*. 2023;180(5):647–666. doi:10.1111/bph.15980
16. Li Y, Li J, Li S, et al. Exploring the gut microbiota's crucial role in acute pancreatitis and the novel therapeutic potential of derived extracellular vesicles. *Front Pharmacol*. 2024;15:1437894. doi:10.3389/fphar.2024.1437894
17. Ammer-Herrmenau C, Antweiler KL, Asendorf T, Beyer G. Gut microbiota predicts severity and reveals novel metabolic signatures in acute pancreatitis. *Gut*. 2024;73(3):485–495. doi:10.1136/gutjnl-2023-330987
18. Rapin A, Pattaroni C, Marsland BJ, Harris NL. Microbiota analysis using an illumina MiSeq platform to sequence 16S rRNA genes. *Curr Protoc Mouse Biol*. 2017;7(2):100–129. doi:10.1002/cpmo.29
19. Yu S, Xiong Y, Fu Y, et al. Shotgun metagenomics reveals significant gut microbiome features in different grades of acute pancreatitis. *Microb Pathog*. 2021;154:104849. doi:10.1016/j.micpath.2021.104849
20. Yu S, Xiong Y, Xu J, et al. Identification of dysfunctional gut microbiota through rectal swab in patients with different severity of acute pancreatitis. *Digestive Dis Sci*. 2020;65(11):3223–3237. doi:10.1007/s10620-020-06061-4
21. Gunathilake M, Lee J, Choi IJ, et al. Alterations in gastric microbial communities are associated with risk of gastric cancer in a korean population: a case-control study. *Cancers*. 2020;12(9):2619. doi:10.3390/cancers12092619
22. Yang C, Mai J, Cao X, Burberry A, Cominelli F. ggpicrust2: an R package for PICRUSt2 predicted functional profile analysis and visualization. *Bioinformatics*. 2023;39(8):btad470. doi:10.1093/bioinformatics/btad470
23. Douglas GM, Maffei VJ, Zaneveld JR. PICRUSt2 for prediction of metagenome functions. *Nature Biotechnol*. 2020;38(6):685–688. doi:10.1038/s41587-020-0548-6
24. Kanehisa M, Furumichi M, Tanabe M, Sato Y, Morishima K. KEGG: new perspectives on genomes, pathways, diseases and drugs. *Nucleic Acids Res*. 2017;45(D1):D353–d361. doi:10.1093/nar/gkw1092
25. Caspi R, Billington R, Ferrer L, et al. The MetaCyc database of metabolic pathways and enzymes and the BioCyc collection of pathway/genome databases. *Nucleic Acids Res*. 2016;44(D1):D471–80. doi:10.1093/nar/gkv1164
26. Šimundić AM. Measures of diagnostic accuracy: basic definitions. *Ejifcc*. 2009;19(4):203–211.
27. Gong L, Li X, Ji L, et al. Characterization and comparison of gut microbiota in patients with acute pancreatitis by metagenomics and culturomics. *Heliyon*. 2025;11(3):e42243. doi:10.1016/j.heliyon.2025.e42243
28. Liu Q, Ruan K, An Z, et al. Updated review of research on the role of the gut microbiota and microbiota-derived metabolites in acute pancreatitis progression and inflammation-targeted therapy. *Int J Biol Sci*. 2025;21(3):1242–1258. doi:10.7150/ijbs.108858
29. Liu X, Mao B. Blautia-a new functional genus with potential probiotic properties? *Gut Microbes*. 2021;13(1):1–21. doi:10.1080/19490976.2021.1875796
30. Martín R, Rios-Covian D, Huillet E, Auger S, Khazaal S, Bermúdez-Humarán LG. Faecalibacterium: a bacterial genus with promising human health applications. *FEMS Microbiol Rev*. 2023;47(4). doi:10.1093/femsre/fuad039
31. Duncan SH, Holtrop G, Lobley GE, Calder AG, Stewart CS, Flint HJ. Contribution of acetate to butyrate formation by human faecal bacteria. *Br J Nutr*. 2004;91(6):915–923. doi:10.1079/bjn20041150
32. Liu H, Wang J, He T, et al. Butyrate: a Double-Edged Sword for Health? *Adv Nutr*. 2018;9(1):21–29. doi:10.1093/advances/nmx009
33. Chen X, Chen X, Yan D. GV-971 prevents severe acute pancreatitis by remodeling the microbiota-metabolic-immune axis. *Nat Commun*. 2024;15(1):8278. doi:10.1038/s41467-024-52398-z
34. Lv X, Zhan L, Ye T, et al. Gut commensal Agathobacter rectalis alleviates microglia-mediated neuroinflammation against pathogenesis of Alzheimer disease. *iScience*. 2024;27(11):111116. doi:10.1016/j.isci.2024.111116
35. hertz S, Anderson JM, Nielsen HL. Fecal microbiota is associated with extraintestinal manifestations in inflammatory bowel disease. *Ann Med*. 2024;56(1):2338244. doi:10.1080/07853890.2024.2338244
36. Olejniczak-Staruch I, Ciążyńska M, Sobolewska-Sztychny D, Narbutt J, Skibińska M, Lesiak A. Alterations of the skin and gut microbiome in psoriasis and psoriatic arthritis. *Int J Mol Sci*. 2021;22(8):3998. doi:10.3390/ijms22083998
37. Boyanova L, Markovska R, Mitov I. Virulence arsenal of the most pathogenic species among the Gram-positive anaerobic cocci, Finegoldia magna. *Anaerobe*. 2016;42:145–151. doi:10.1016/j.anaerobe.2016.10.007
38. Brown K, Church D, Lynch T, Gregson D. Bloodstream infections due to Peptoniphilus spp.: report of 15 cases. *Clin Microbiol Infect*. 2014;20(11):O857–60. doi:10.1111/1469-0691.12657
39. Morand A, Tall ML, Kuete Yimagou E, et al. Anaerococcus urinimassiliensis sp. nov. a new bacterium isolated from human urine. *Sci Rep*. 2021;11(1):2684. doi:10.1038/s41598-021-82420-z

40. Medawar E, Haange SB, Rolle-Kampczyk U. Gut microbiota link dietary fiber intake and short-chain fatty acid metabolism with eating behavior. *Transl Psychiatr*. 2021;11(1):500. doi:10.1038/s41398-021-01620-3
41. Liu J, Qiu H, Zhao J, et al. Parabacteroides as a promising target for disease intervention: current stage and pending issues. *NPJ Biofilms Microbiomes*. 2025;11(1):137. doi:10.1038/s41522-025-00772-0
42. Glascock AL, Jimenez NR, Boundy S, et al. Unique roles of vaginal Megasphaera phylotypes in reproductive health. *Microb Genom*. 2021;7(12). doi:10.1099/mgen.0.000526
43. Efremova I, Alieva A, Maslennikov R, et al. Akkermansia muciniphila is associated with normal muscle mass and Eggerthella is related with sarcopenia in cirrhosis. *Front Nutr*. 2024;11:1438897. doi:10.3389/fnut.2024.1438897
44. Tran NTD, Chaidee A, Surapinit A, et al. Strongyloides stercoralis infection reduces Fusicatenibacter and Anaerostipes in the gut and increases bacterial amino-acid metabolism in early-stage chronic kidney disease. *Heliyon*. 2023;9(9):e19859. doi:10.1016/j.heliyon.2023.e19859
45. Tsai CC, Chiu MH, Kek HP. The reduced gut lachnospira species is linked to liver enzyme elevation and insulin resistance in pediatric fatty liver disease. *Int J Mol Sci*. 2024;25(7):3640. doi:10.3390/ijms25073640
46. Ling ZN, Jiang YF, Ru JN, Lu JH, Ding B, Wu J. Amino acid metabolism in health and disease. *Signal Transduction Targeted Ther*. 2023;8(1):345. doi:10.1038/s41392-023-01569-3
47. Wang N, Wang B, Maswikiti EP, et al. AMPK-a key factor in crosstalk between tumor cell energy metabolism and immune microenvironment? *Cell Death Discovery*. 2024;10(1):237. doi:10.1038/s41420-024-02011-5
48. Cui Y, Chen J, Zhang Z, Shi H, Sun W, Yi Q. The role of AMPK in macrophage metabolism, function and polarisation. *J Transl Med*. 2023;21(1):892. doi:10.1186/s12967-023-04772-6
49. Roach PJ, Depaoli-Roach AA, Hurley TD, Tagliabracci VS. Glycogen and its metabolism: some new developments and old themes. *Biochem J*. 2012;441(3):763–787. doi:10.1042/bj20111416
50. Rigatti SJ. Random Forest. *J Insur Med*. 2017;47(1):31–39. doi:10.17849/insm-47-01-31-39.1
51. Breiman L. Random forests. *Machine Learning*. 2001;45(1):5–32. doi:10.1023/A:1010933404324
52. Song M, Jung H, Lee S, Kim D, Ahn M. Diagnostic classification and biomarker identification of alzheimer's disease with random forest algorithm. *Brain Sci*. 2021;11(4):453. doi:10.3390/brainsci11040453
53. Cutler DR, Edwards TC, Beard KH, et al. Random forests for classification in ecology. *Ecology*. 2007;88(11):2783–2792. doi:10.1890/07-0539.1